



HAL
open science

Size effect on single pulse all-optical helicity-independent switching in GdFeCo disk arrays

Danny Petty Gweha Nyoma, Maxime Vergès, Michel Hehn, Daniel Lacour, Julius Hohlfeld, Sebastiaan van Dijken, Grégory Malinowski, Stéphane Mangin, François Montaigne

► To cite this version:

Danny Petty Gweha Nyoma, Maxime Vergès, Michel Hehn, Daniel Lacour, Julius Hohlfeld, et al.. Size effect on single pulse all-optical helicity-independent switching in GdFeCo disk arrays. Applied Physics Letters, 2023, 123 (5), pp.052405. 10.1063/5.0150250 . hal-04244267

HAL Id: hal-04244267

<https://hal.science/hal-04244267>

Submitted on 17 Oct 2023

HAL is a multi-disciplinary open access archive for the deposit and dissemination of scientific research documents, whether they are published or not. The documents may come from teaching and research institutions in France or abroad, or from public or private research centers.

L'archive ouverte pluridisciplinaire **HAL**, est destinée au dépôt et à la diffusion de documents scientifiques de niveau recherche, publiés ou non, émanant des établissements d'enseignement et de recherche français ou étrangers, des laboratoires publics ou privés.

Copyright

RESEARCH ARTICLE | AUGUST 01 2023

Size effect on single pulse all-optical helicity-independent switching in GdFeCo disk arrays

Danny Petty Gweha Nyoma ; Maxime Vergès ; Michel Hehn ; Daniel Lacour ; Julius Hohfeld ; Sebastiaan van Dijken ; Grégory Malinowski ; Stéphane Mangin ; François Montaigne  

 Check for updates

Appl. Phys. Lett. 123, 052405 (2023)

<https://doi.org/10.1063/5.0150250>



View Online



Export Citation

CrossMark

Articles You May Be Interested In

Evolution of switching fields caused by reorientation of GdFeCo/Ir/GdFeCo synthetic ferrimagnet in magnetic field

J. Appl. Phys. (March 2023)

Field-free current-induced magnetization switching in GdFeCo: A competition between spin-orbit torques and Oersted fields

J. Appl. Phys. (August 2022)

Novel behaviors of coercivity in GdFeCo/Hf/MgO heterostructure

AIP Advances (April 2022)

17 October 2023 08:40:14



Cut Hall measurement time in *half* using an M91 FastHall™ controller



Also available as part of a tabletop system and an option for your PPMS® system

Size effect on single pulse all-optical helicity-independent switching in GdFeCo disk arrays

Cite as: Appl. Phys. Lett. **123**, 052405 (2023); doi: [10.1063/5.0150250](https://doi.org/10.1063/5.0150250)

Submitted: 13 March 2023 · Accepted: 13 July 2023 ·

Published Online: 1 August 2023



View Online



Export Citation



CrossMark

Danny Petty Gweha Nyoma,¹ Maxime Vergès,¹ Michel Hehn,¹ Daniel Lacour,¹ Julius Hohlfeld,¹ Sebastiaan van Dijken,² Grégory Malinowski,¹ Stéphane Mangin,¹ and François Montaigne^{1,a)}

AFFILIATIONS

¹Université de Lorraine, CNRS, IJL, F-54000 Nancy, France

²NanoSpin, Department of Applied Physics, Aalto University School of Science, FI-00076 Aalto, Finland

^{a)} Author to whom correspondence should be addressed: francois.montaigne@univ-lorraine.fr

ABSTRACT

We experimentally demonstrate single pulse toggle switching of the magnetization of GdFeCo disks with perpendicular to film plane anisotropy, which diameter ranges from 3 μm to 400 nm using 35 fs linearly polarized laser pulses. Two different magnetic states can be observed depending on the laser fluence: either a deterministic switching of the disk magnetization or a randomly oriented disk. We report that the fluence required to observe both magnetic states show a non-monotonic behavior with disk diameter and that the smallest disks require the lowest minimum fluence for achieving single pulse all-optical helicity-independent switching. Different evolution of the fluence thresholds for both phenomenon as a function of the disk size is observed and discussed.

Published under an exclusive license by AIP Publishing. <https://doi.org/10.1063/5.0150250>

Achieving control of magnetization at smaller length and faster time scales is the horizon of research in nano-magnetism. This interest stems from the ever-increasing need to decrease the reading and writing rate of magnetic memory devices, which are made of nanosized magnetic bits. For the manipulation of magnetism at the 100 ps time-scale, several efficient techniques (spin-polarized charge currents,^{1,2} electric fields,³ and THz pulses⁴) have been developed. One particular method is to use femtosecond laser pulses to demagnetize⁵ but also to deterministically switch^{6–11} the magnetization of magnetic materials. For magnetic recording application, single laser pulse turned out to be a good candidate due to the demonstration of ultrafast single pulse all optical helicity independent switching (AO-HIS) in particular materials. In 2011, Radu *et al.* reported the first observation of AO-HIS in GdFeCo ferrimagnetic amorphous alloys.¹² Since then, experimental observations of single pulse AO-HIS have been confirmed in this ferrimagnetic material^{13,14} and have also been demonstrated in several other magnetic materials, such as spin-valve structure,^{15–17} rare-earth-free Heusler alloy $\text{Mn}_2\text{Ru}_x\text{Ga}$,¹⁸ Pt/Co/Pt tri-layer, and TbCo alloys doped with small amount of Gd,^{19–21} Gd/Co,²² and Tb/Co synthetic ferrimagnets.^{23–25}

The magnetization reversal in GdFeCo alloys, made of two antiferromagnetically coupled sublattices of rare-earth and transition metal, can be understood as the excitation of electrons by absorption of photons allowing demagnetization at different rates

of the two sublattices thanks to the Elliott–Yafet effect and exchange scattering.⁵ The difference in demagnetization rates leads to a transient ferromagnetic-like-state that end by a complete ultrafast reversal of the magnetization by conservation of angular momentum.^{12,26,27} Those models based on angular momentum conservation describe the purely heat-driven toggle switching. This phenomenon has been intensively studied in GdFeCo full films with perpendicular anisotropy^{6,14,28–30} but studies on the influence of reduced lateral size remain limited.^{31–34} Particularly, El-Ghazaly *et al.*³⁴ demonstrated AO-HIS in amorphous submicrometric GdCo dots and showed that the reversing time is significantly reduced for dots below 500 nm compared to 15 μm squares. They explained this faster rate by the electron–phonon and spin-lattice interactions. In view of these previous works, question like the behavior of the threshold fluence to observe switching in GdFeCo magnetic out of plane nanostructures remains open.

In this Letter, we present a systematic study of the magnetization reversal for GdFeCo disks whose diameter ranges from 3 μm to 400 nm illuminated by 35 fs linearly polarized laser pulses. Toggle switching was observed for all sizes, and switching/random threshold fluencies were precisely determined. The dependence of both thresholds on disk size revealed a non-monotonic behavior, which highlights the importance of the specific light absorption in nanostructures. Moreover, the influence of the period for 400 nm disks arrays was

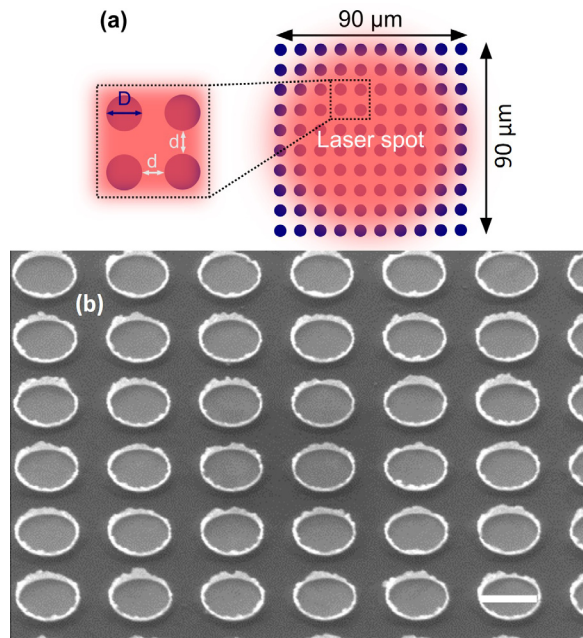


FIG. 1. Design of the sample. (a) Sketch of $90 \times 90 \mu\text{m}^2$ areas filled with patterned disks of diameter D and fixed spacing d equal to 300 nm. The red circle represents the laser spot of the incident beam centered on the disk array. (b) Scanning electron microscopy (SEM) image with 45° tilt showing good agreement of the pitch and the diameter in a region of 400 nm disk array. The length of the scale bar is 400 nm.

investigated and numerical simulations could reproduce the non-monotonic behavior.

The sample namely glass (substrate)//Ta (5 nm)/Cu (5 nm)/ $\text{Gd}_{24}(\text{FeCo})_{76}$ (20 nm)/Pt (5 nm) was grown by magnetron sputtering. The full film exhibits both perpendicular magnetic anisotropy (PMA) and single shot AO-HIS at room temperature. To study the size effect, we fabricated arrays of magnetic disks with diameter ranging from $3 \mu\text{m}$ down to 400 nm. The magnetic film has been processed by ion

beam etching through an aluminum mask defined by electron-beam lithography and lift-off. The remaining Al mask is subsequently removed by chemical etching. As illustrated in Fig. 1, for each disk diameter D , $90 \times 90 \mu\text{m}^2$ areas are filled with identical disks on a square lattice. The distance between disks d is fixed to 300 nm (the lattice period is, therefore, not constant and equal to $D + d$). The effect of the excitation by 35 fs laser pulse generated by a Ti-sapphire laser on the magnetic nanostructures is characterized *in situ* by magneto-optic Kerr effect (MOKE) microscopy. This laser delivers 800 nm wavelength laser pulses, linearly polarized after propagating through a Glan-Taylor polarizer. The number of laser pulses and the repetition rate can be modified by using a pulse picker. In this work, we have only use single pulse exposition (two pulses results are obtained manually with more than 1 s between the two pulses). Pulse power can be changed by using the combination of the half-wave plate and the Glan-Taylor polarizer. A convex lens focuses the beam with a Gaussian intensity profile onto the sample surface down to a full-width half-maximum (FWHM) of $69 \pm 0.5 \mu\text{m}$. This spot diameter is chosen to ensure a switching region smaller than the $90 \mu\text{m}$ magnetic array width to be able to measure the switching domain of a single array of disks.

Figure 2 shows the AO-HIS results for arrays of $\text{Gd}_{24}(\text{FeCo})_{76}$ disks initially saturated. A 1 T out of plane applied field is first applied such that initial magnetization in the disks is pointing down corresponding to the light gray color [Fig. 2(a)]. After excitation with a first pulse, one can see the formation of a dark-gray area independently of the disk sizes. A second identical pulse subsequently, shined at the same position with a delay of about one second, reverses the magnetization back to the initial state forming a light gray area. By starting from the opposite magnetic direction [Fig. 2(b)], we observed the same behavior. Regardless of the initial disk magnetization direction, after the second femtosecond laser pulse, a ring is formed. These rings are obtained for all disks sizes and appear larger for smaller disks. This ring highlights that in an intermediate range of fluence, the reversing presents a stochastic aspect. This stochastic aspect appears more important for smaller disks. These aspects are beyond the scope of this Letter. These experimental results demonstrate AO-HIS for all the GdFeCo disk diameters ranging from $3 \mu\text{m}$ to 400 nm after a single 35 fs linearly polarized laser pulse. Moreover, Fig. 2 presents a non-

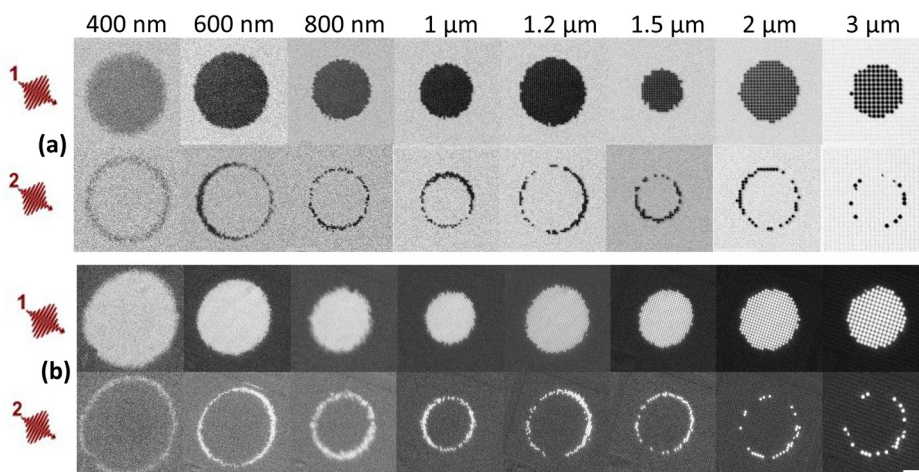


FIG. 2. Magneto-optical images of magnetic disks made of $\text{Gd}_{24}(\text{FeCo})_{76}$ obtained after the action of one 35 fs linearly polarized pulse and then a second pulse separated by 1 s. Initially, disk arrays are saturated in the (a) downward and (b) upward direction with a 1 T out of plane applied field. The dark gray (light gray) area represents magnetization of disks pointing "up" ("down"). Each laser pulse with a fluence of $17.7 \text{ mJ}/\text{cm}^2$ irradiates the same circular region of the patterned structure and reverses the magnetization within it. The length of the scale bar is $20 \mu\text{m}$.

monotonic behavior of the switched area size with the disk diameter for a given fluence.

In a second step, the impact of the laser fluence on the switched area has been studied as function of disk size. Therefore, we systematically irradiated each array with eight different fluences and measured the switching/random domain sizes by using a MOKE microscope. Figure 3 presents the magnetic state of GdFeCo disk arrays after excitation with a single femtosecond laser pulse. Initially, the arrays were saturated perpendicular with a 1 T field, as previously done in Fig. 2. On the MOKE images, one can observe up to three different magnetic states depending on the pulse energy: no switching, deterministic switching, and randomly oriented disk. For example, in the case of disks with 800 nm diameter, no effect of light on disks is observed for fluence below 14.5 mJ/cm² (no switching state) [Fig. 3(a)], magnetization reversal is achieved for pulses energies between 14.5 and 19.2 mJ/cm² (deterministic switching) [Figs. 3(b)–3(e)] within a circular zone of diameter D_{sw} . For larger fluence around 20.8 mJ/cm², at the center, the array of disk is no longer uniformly magnetized [Fig. 3(f)]. This central zone of diameter D_{ra} is marked by two possible magnetic configurations of a disk depending on its size. Indeed, we only observed disks with a single uniform randomly oriented domains for disks up to 1 μm of diameter. While for disks larger than 1 μm, single uniform randomly oriented domains and multidomain states are observed. (Supplementary material shows the magnetic state of individual GdFeCo disk for the data in Fig. 3). For each disk size, the

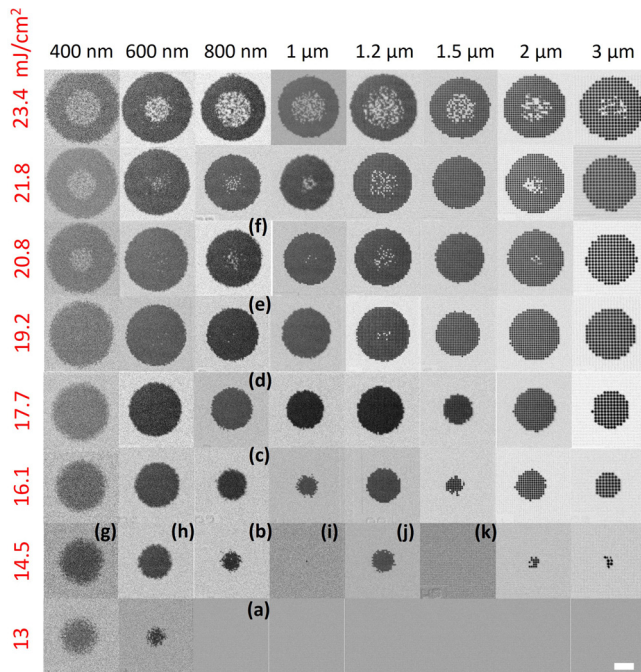


FIG. 3. Magneto-optical images of Gd₂₄(FeCo)₇₆ magnetic disks obtained after a single 35 fs laser pulse, linearly polarized. Depending on the fluence and the disk diameter, we observe three different magnetic states: (a) light gray area for no switching at low pulse fluence, (b)–(e) homogenous dark gray area for AO-HIS at medium energy, and (f) non-homogenous dark gray area for randomly oriented disks at the center of the laser spot for high pulse fluence. The length of the scale bar is 20 μm.

diameter of the switched/random region increases with laser pulse energy but for a given fluence, D_{sw} and D_{ra} depend on the disk size. Qualitatively, at the same fluence, we observe a non-monotonic behavior of the switching domain surface with the disk size. [For instance, although 14.5 mJ/cm² is sufficient to induce AO-HIS in 400 nm, 600 nm, 800 nm, and 1.2 μm disks, as shown in Figs. 3(g), 3(h), 3(b), and 3(j), respectively, this fluence is too low to affect the magnetization of 1 and 1.5 μm disks, as shown in Figs. 3(i) and 3(k) respectively].

For a deeper analysis, we measured the switching/random diameters and considered a Gaussian distribution of the laser intensity to determine the threshold fluencies for AO-HIS and randomized state (see more details in supplementary material). For each disk diameter, F_{sw} and F_{ra} have been determined using a single value of $D_L = 68.4 \pm 0.6 \mu\text{m}$, value which is consistent with the direct measure of the beam diameter ($69 \pm 0.5 \mu\text{m}$). We plot in Fig. 4(a) a state diagram for GdFeCo disk arrays illuminated by 35 fs linearly polarized laser pulses where we indicate the dependence of threshold fluencies for switched F_{sw} and randomized F_{ra} state on disk diameter. Quantitatively, we observe three different magnetic states: no switching for low fluence, random oriented disk at high fluence and magnetization reversal between these two. While F_{sw} and F_{ra} have a global tendency to increase with disk diameter, the details of the state diagram indicate a non-monotonic behavior.

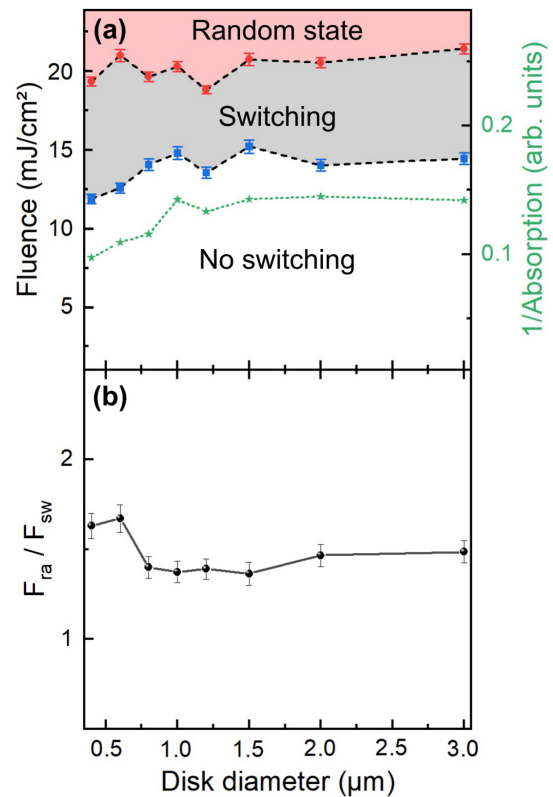


FIG. 4. AO-HIS state diagram of Gd₂₄(FeCo)₇₆ disks. Evolution of (a) the threshold fluence for switching (random) state F_{sw} (F_{ra}), the calculated inverse of the absorbance and (b) the fluence ratio F_{ra}/F_{sw} as function of disk diameter depicted in blue squares (red dots), green stars, and black dots, respectively.

Finally, we studied the influence of the period on the threshold fluence for periodic GdFeCo nanostructures made of 400 nm disks diameter. Therefore, we systematically excited with a single 35 fs laser pulse and looked to the reversal in arrays with 100, 150, 200, 300, 400, and 500 nm spacing between the disks. By measuring the diameter of the switched area within an optical microscope for each periodic arrays, we can extract the threshold fluence for each lattice period. Figure 5 shows the variation of the threshold fluence extracted from MOKE images as a function of the 400 nm disk arrays period. This figure shows that the switching threshold also depends on the spacing/period varying non monotonically between 9.7 and 12.8 mJ/cm² for spacings ranging from 100 to 500 nm. Since toggle switching can be achieved for closer nano-disks, we conclude that magnetostatic coupling between nanostructures does not play a huge role on ultrafast optical switching in periodic GdFeCo nano-disks. Moreover, Fig. 5 shown that closer nano-disks need less energy to cause AOS and present a non-monotonic behavior of the threshold fluence with the period/spacing. The size range of the threshold fluence variations and their non-monotonicity suggests a predominant influence of the wave nature of light and its finite wavelength.

We performed simulations with COMSOL Multiphysics with the module *Wave Optics* to calculate the absorbed energy for different geometries of the periodic arrays of magnetic nano-disks for the same light power fixed to 0.16 μ W. This way we wanted to check out if the non-monotonic evolution of threshold fluence with disk diameter is consistent or not with the evolution of the energy absorption as a function of the disk diameter and the period of the array.³⁵ We considered periodic arrays of magnetic nano-disks with $D = 400, 600, 800, 1000, 1200, 1500, 2000,$ and 3000 nm with corresponding lattice period $P = 700, 900, 1100, 1300, 1500, 1800, 2300,$ and 3300 nm for keeping the same edge-to-edge distance between two neighboring disks. The thin film stack considered is namely glass (substrate)//Ta (5 nm)/Cu (5 nm)/Gd₂₄(FeCo)₇₆(20 nm)/Pt (5 nm) as for the experimental measurements. We considered a glass substrate and air superstrate with

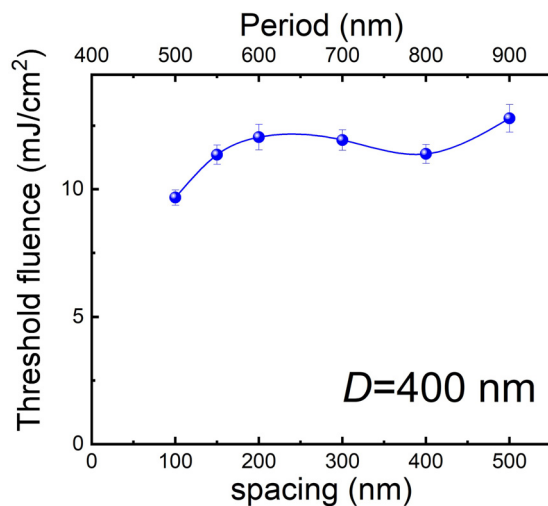


FIG. 5. Threshold switching fluence on 400 nm Gd₂₄(FeCo)₇₆ disks as a function of the period/spacing.

refractive indices of 1.5 and 1, respectively. Concerning the metals, we used the refractive indices from Ref. 36 for Ta and Pt while we used the data sets from Refs. 37 and 38 for Cu and GdFeCo. This specific numerical method considers one unit cell that is why we applied periodic boundary conditions (Floquet periodicity) on its edges to simulate the electromagnetic field distribution in periodic arrangements of GdFeCo nano-disks. The source comes in from the air superstrate at normal incidence and comes out from the glass substrate. To avoid unphysical reflections, perfect matched layer domains on top of air domain and at the bottom of glass substrate were considered. The source is a monochromatic linearly polarized plane wave with p polarization. The wavelength is fixed at 800 nm. The mesh is made of free triangular elements whose maximum size was 2 nm. This method provides the total absorption of the system {air + periodic arrays of nano-disks + glass}, but since air and glass are assumed to absorb no energy, this provides the absorption of the periodic array. To describe the local absorption of light, we scaled any calculated total absorption by the filling factor of the periodic array. We calculated the absorption of the continuous films with the same approach. (Here, the filling factor is 100%.)

Figure 4 shows (for different scales) the experimental results and the calculated inverse of the absorbance, which should be proportional to the switching and random threshold fluence. The good qualitative agreement is obtained since the simulations reproduce the decrease in the switching and random fluences for small diameters. Furthermore, the non-monotonic variation of the switching fluence is well described while the agreement is not as good for the random threshold fluence. If both phenomena differ by the physics involved and particularly occurs at different timescales, they are believed to be due to the heat assisted effect which are directly related to the absorbed energy. Within this picture, if the disk size only influences only the proportion of incident energy transferred to the nanostructure, the ratio between the random and switching threshold fluences is expected to be constant. This is not experimentally confirmed as shown in Fig. 4(b).

The limit of the previous analysis, considering an averaged energy at the scale of the disk, is certainly the non-uniform energy absorption within the magnetic nanostructure. The supplementary material gives some examples of the spatial variation of the energy absorption. Variations up to a factor of 3 are predicted. Similar absorption profiles have been predicted in GdFeCo microstructures when the disk size is smaller than the beam diameter, due to the formation of a standing wave pattern caused by scattering of the light from the edges of the structure.³¹ This non uniform energy repartition would lead to non-uniform temperature and locally different magnetic processes. In that case, it is possible at some fluence that part of the structure experiences a magnetization reversal, whereas another part is multidomain. The final configuration would result from a complex process involving micromagnetism and the evolving temperature field.

In conclusion, we demonstrated that GdFeCo magnetic micro- and nano-disk can be switched deterministically with a single ultrafast laser pulse for a range of fluence. For larger laser fluence, the magnetic disk is randomly oriented up or down. The threshold fluences for the two types of switching evolve non-monotonically with disk size. Numerical simulations that highlight the creation of standing waves induced by light scattering giving a non-uniform distribution of absorption within the disks could reproduce the non-monotonic behavior of both fluence thresholds. These results will contribute to

further developments of strategies for deterministic light control of magnetization at the nanoscale.

See the supplementary material that shows a zoom of the magnetic state of individual GdFeCo disk after laser pulse irradiation, a detailed methodology describing the extraction of the laser beam diameter and the threshold fluences, and the illustration of the non-homogenous light absorption.

This work was supported partly by the French PIA project “Lorraine Université d’Excellence” (No. ANR-15-IDEX-04-LUE) and by the “FEDER-FSE Lorraine et Massif Vosges 2014–2020,” a European Union Program (RaNGE project). This work was supported by the No. ANR-20-CE09-0013 UFO, by the Institute Carnot ICEEL for the project “CAPMAT” and FASTNESS, by the Région Grand Est, by the Metropole Grand Nancy, for the Chaire PLUS by the European Union’s Horizon 2020 research and innovation program COMRAD under the Marie Skłodowska-Curie Grant Agreement No. 861300, and by the Academy of Finland (Grant No. 316857). This article is based upon work from COST Action CA17123 MAGNETOFON, supported by COST (European Cooperation in Science and Technology). Devices in the present study were patterned at MiNaLor clean-room platform, which is partially supported by FEDER and Grand Est Region through the RaNGE project.

AUTHOR DECLARATIONS

Conflict of Interest

The authors have no conflicts to disclose.

Author Contributions

Danny Petty Gweha Nyoma: Formal analysis (equal); Investigation (lead); Writing – original draft (lead). **Maxime Verges:** Investigation (supporting); Visualization (equal); Writing – review & editing (equal). **Michel Hehn:** Conceptualization (equal); Investigation (equal); Writing – review & editing (equal). **Daniel Lacour:** Conceptualization (equal); Writing – review & editing (equal). **Julius Hohlfeld:** Conceptualization (equal); Investigation (equal). **Sebastian van Dijken:** Writing – review & editing (equal). **Gregory Malinowski:** Conceptualization (equal); Investigation (equal); Methodology (equal); Validation (equal); Writing – review & editing (equal). **Stéphane Mangin:** Conceptualization (equal); Funding acquisition (equal); Validation (equal); Writing – original draft (equal); Writing – review & editing (equal). **François Montaigne:** Formal analysis (equal); Methodology (equal); Supervision (equal); Writing – original draft (supporting); Writing – review & editing (equal).

Data Availability

The data that support the findings of this study are available from the corresponding author upon reasonable request.

REFERENCES

¹S. Krause, L. Berbil-Bautista, G. Herzog, M. Bode, and R. Wiesendanger, *Science* **317**, 1537–1540 (2007).

- ²L. Liu, Q. Qin, W. Lin, C. Li, Q. Xie, S. He, X. Shu, C. Zhou, Z. Lim, J. Yu, W. Lu, M. Li, X. Yan, S. J. Pennycook, and J. Chen, *Nat. Nanotechnol.* **14**, 939–944 (2019).
- ³T. Lottermoser, T. Lonkai, U. Amann, D. Hohlwein, J. Ihringer, and M. Fiebig, *Nature* **430**, 541–544 (2004).
- ⁴T. Kubacka, J. A. Johnson, M. C. Hoffmann, C. Vicario, S. de Jong, P. Beaud, S. Grübel, S.-W. Huang, L. Huber, L. Patthey, Y.-D. Chuang, J. J. Turner, G. L. Dakovski, W.-S. Lee, M. P. Miniti, W. Schlotter, R. G. Moore, C. P. Hauri, S. M. Koohpayeh, V. Scagnoli, G. Ingold, S. L. Johnson, and U. Staub, *Science* **343**, 1333–1336 (2014).
- ⁵E. Beaurepaire, J.-C. Merle, A. Daunois, and J.-Y. Bigot, *Phys. Rev. Lett.* **76**, 4250–4253 (1996).
- ⁶D. Stanciu, F. Hansteen, A. V. Kimel, A. Kirilyuk, A. Tsukamoto, A. Itoh, and T. Rasing, *Phys. Rev. Lett.* **99**, 047601 (2007).
- ⁷S. Mangin, M. Gottwald, C.-H. Lambert, D. Steil, V. Uhlir, L. Pang, M. Hehn, S. Alebrand, M. Cinchetti, G. Malinowski, Y. Fainman, M. Aeschlimann, and E. E. Fullerton, *Nat. Mater.* **13**, 286–292 (2014).
- ⁸C.-H. Lambert, S. Mangin, B. S. D. C. S. Varaprasad, Y. K. Takahashi, M. Hehn, M. Cinchetti, G. Malinowski, K. Hono, Y. Fainman, M. Aeschlimann, and E. E. Fullerton, *Science* **345**, 1337–1340 (2014).
- ⁹G. Kichin, M. Hehn, J. Gorchon, G. Malinowski, J. Hohlfeld, and S. Mangin, *Phys. Rev. Appl.* **12**, 024019 (2019).
- ¹⁰Q. Remy, J. Igarashi, S. Iihama, G. Malinowski, M. Hehn, J. Gorchon, J. Hohlfeld, S. Fukami, H. Ohno, and S. Mangin, *Adv. Sci.* **7**, 2001996 (2020).
- ¹¹J. Igarashi, Q. Remy, S. Iihama, G. Malinowski, M. Hehn, J. Gorchon, J. Hohlfeld, S. Fukami, H. Ohno, and S. Mangin, *Nano Lett.* **20**, 8654–8660 (2020).
- ¹²I. Radu, K. Vahaplar, C. Stamm, T. Kachel, N. Pontius, H. A. Dürr, T. A. Ostler, J. Barker, R. F. L. Evans, R. W. Chantrell, A. Tsukamoto, A. Itoh, A. Kirilyuk, T. Rasing, and A. V. Kimel, *Nature* **472**, 205–208 (2011).
- ¹³J. Wei, B. Zhang, M. Hehn, W. Zhang, G. Malinowski, Y. Xu, W. Zhao, and S. Mangin, *Phys. Rev. Appl.* **15**, 054065 (2021).
- ¹⁴Y. Xu and S. Mangin, *J. Magn. Magn. Mater.* **564**, 170169 (2022).
- ¹⁵S. Iihama, Y. Xu, M. Deb, G. Malinowski, M. Hehn, J. Gorchon, E. E. Fullerton, and S. Mangin, *Adv. Mater.* **30**(51), 1804004 (2018).
- ¹⁶J. Gorchon, M. Hehn, G. Malinowski, and S. Mangin, *J. Magn. Magn. Mater.* **563**, 169919 (2022).
- ¹⁷Q. Remy, J. Hohlfeld, M. Vergès, Y. Le Guen, J. Gorchon, G. Malinowski, S. Mangin, and M. Hehn, *Nat. Commun.* **14**(1), 445 (2023).
- ¹⁸C. Banerjee, N. Teichert, K. E. Siewierska, Z. Gercsi, G. Y. P. Atcheson, P. Stamenov, K. Rode, J. M. D. Coey, and J. Besbas, *Nat. Commun.* **11**, 4444 (2020).
- ¹⁹D. P. G. Nyoma, M. Hehn, G. Malinowski, J. Hohlfeld, J. Gorchon, S. Mangin, and F. Montaigne, “Gd doping at the Co/Pt interfaces to induce ultra-fast all-optical switching” (unpublished).
- ²⁰A. Ceballos, A. Pattabi, A. El-Ghazaly, S. Ruta, C. P. Simon, R. F. L. Evans, T. Ostler, R. W. Chantrell, E. Kennedy, M. Scott, J. Bokor, and F. Hellman, *Phys. Rev. B* **103**(2), 024438 (2021).
- ²¹W. Zhang, J. X. Lin, T. X. Huang, G. Malinowski, M. Hehn, Y. Xu, S. Mangin, and W. Zhao, *Phys. Rev. B* **105**(5), 054410 (2022).
- ²²M. L. M. Lalieu, M. J. G. Peeters, S. R. R. Haenen, R. Lavrijsen, and B. Koopmans, *Phys. Rev. B* **96**, 220411(R) (2017).
- ²³L. Avilés-Félix, L. Álvaro-Gómez, G. Li, C. S. Davies, A. Olivier, M. Rubio-Roy, S. Auffret, A. Kirilyuk, A. V. Kimel, T. Rasing, L. D. Buda-Prejbeanu, R. C. Sousa, B. Dieny, and I. L. Prejbeanu, *AIP Adv.* **9**, 125328 (2019).
- ²⁴L. Avilés-Félix, A. Olivier, G. Li, C. S. Davies, L. Álvaro-Gómez, M. Rubio-Roy, S. Auffret, A. Kirilyuk, A. V. Kimel, T. Rasing, L. D. Buda-Prejbeanu, R. C. Sousa, B. Dieny, and I. L. Prejbeanu, *Sci. Rep.* **10**, 5211 (2020).
- ²⁵Y. Peng, D. Salomoni, G. Malinowski, W. Zhang, J. Hohlfeld, L. D. Buda-Prejbeanu, J. Gorchon, M. Vergès, J. X. Lin, R. C. Sousa, I. L. Prejbeanu, S. Mangin, and M. Hehn, “In plane reorientation induced single laser pulse magnetization reversal in rare-earth based multilayer,” arXiv [cond-mat.mtrl-sci] (2022).

- ²⁶S. Wienholdt, D. Hinzke, K. Carva, P. M. Oppeneer, and U. Nowak, *Phys. Rev. B* **88**, 020406(R) (2013).
- ²⁷A. M. Kalashnikova and V. I. Kozub, *Phys. Rev. B* **93**, 054424 (2016).
- ²⁸T. A. Ostler, J. Barker, R. F. L. Evans, R. W. Chantrell, U. Atxitia, O. Chubykalo-Fesenko, S. El Moussaoui, L. Le Guyader, E. Mengotti, L. J. Heyderman, F. Nolting, A. Tsukamoto, A. Itoh, D. Afanasiev, B. A. Ivanov, A. M. Kalashnikova, K. Vahaplar, J. Mentink, A. Kirilyuk, T. Rasing, and A. V. Kimel, *Nat. Commun.* **3**(1), 666 (2012).
- ²⁹M. S. El Hadri, P. Pirro, C.-H. Lambert, S. Petit-Watelot, Y. Quessab, M. Hehn, F. Montaigne, G. Malinowski, and S. Mangin, *Phys. Rev. B* **94**, 064412 (2016).
- ³⁰M. Beens, M. L. M. Lalieu, A. J. M. Deenen, R. A. Duine, and B. Koopmans, *Phys. Rev. B* **100**, 220409(R) (2019).
- ³¹M. Savoini, R. Medapalli, B. Koene, A. R. Khorsand, L. Le Guyader, L. Duò, M. Finazzi, A. Tsukamoto, A. Itoh, F. Nolting, A. Kirilyuk, A. V. Kimel, and T. Rasing, *Phys. Rev. B* **86**, 140404(R) (2012).
- ³²L. Le Guyader, S. El Moussaoui, M. Buzzi, R. V. Chopdekar, L. J. Heyderman, A. Tsukamoto, A. Itoh, A. Kirilyuk, T. Rasing, A. V. Kimel, and F. Nolting, *Appl. Phys. Lett.* **101**, 022410 (2012).
- ³³L. Le Guyader, M. Savoini, S. El Moussaoui, M. Buzzi, A. Tsukamoto, A. Itoh, A. Kirilyuk, T. Rasing, A. V. Kimel, and F. Nolting, *Nat. Commun.* **6**, 5839 (2015).
- ³⁴A. El-Ghazaly, B. Tran, A. Ceballos, C.-H. Lambert, A. Pattabi, S. Salahuddin, F. Hellman, and J. Bokor, *Appl. Phys. Lett.* **114**, 232407 (2019).
- ³⁵M. Vergès, S. Perumbilavil, J. Hohlfeld, F. Freire-Fernández, Y. Le Guen, N. Kuznetsov, F. Montaigne, G. Malinowski, D. Lacour, M. Hehn, S. van Dijken, and S. Mangin, *Adv. Sci.* **10**, 2204683 (2023).
- ³⁶W. S. M. Werner, K. Glantschnig, and C. AMBrosch-Draxl, *J. Phys. Chem. Ref. Data* **38**, 1013–1092 (2009).
- ³⁷P. B. Johnson and R. W. Christy, *Phys. Rev. B* **6**, 4370 (1972).
- ³⁸W. R. Hendren, R. Atkinson, R. J. Pollard, I. W. Salter, C. D. Wright, W. W. Clegg, and D. F. L. Jenkins, *J. Phys. Condens. Matter* **15**, 1461 (2003).